XVI конференция «Математические модели и численные методы в биологии и медицине»
Институт вычислительной математики им. Г.И. Марчука РАН

Пространственное распределение и транспорт опсина в наружном сегменте фоторецепторов-колбочек

А.А. Токарев

Институт химической физики им. Н.Н.Семёнова РАН

1 ноября 2024

Anatomy of the human eye and photoreceptor morphology

Hussey et al, 2022

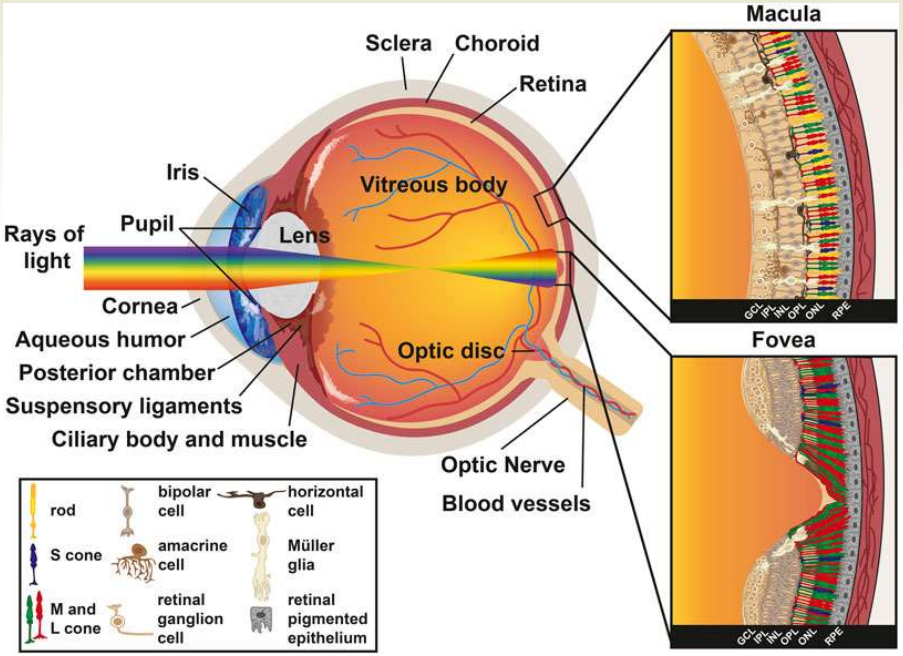

Hussey et al, 2022

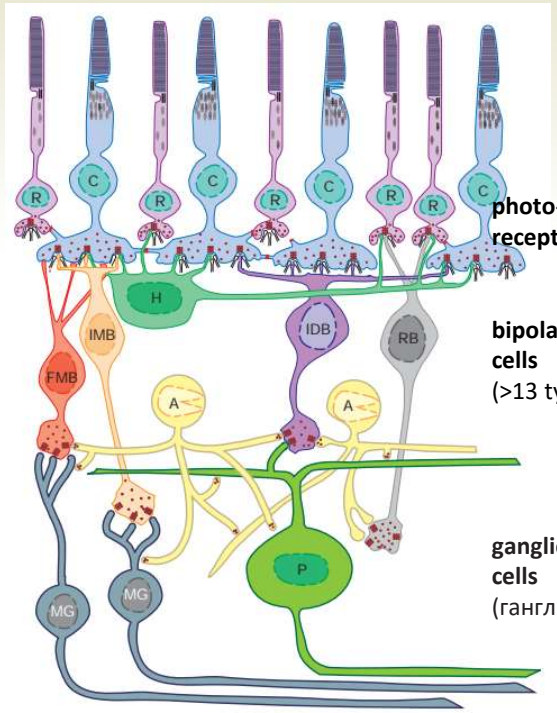

Squire et al, 2008

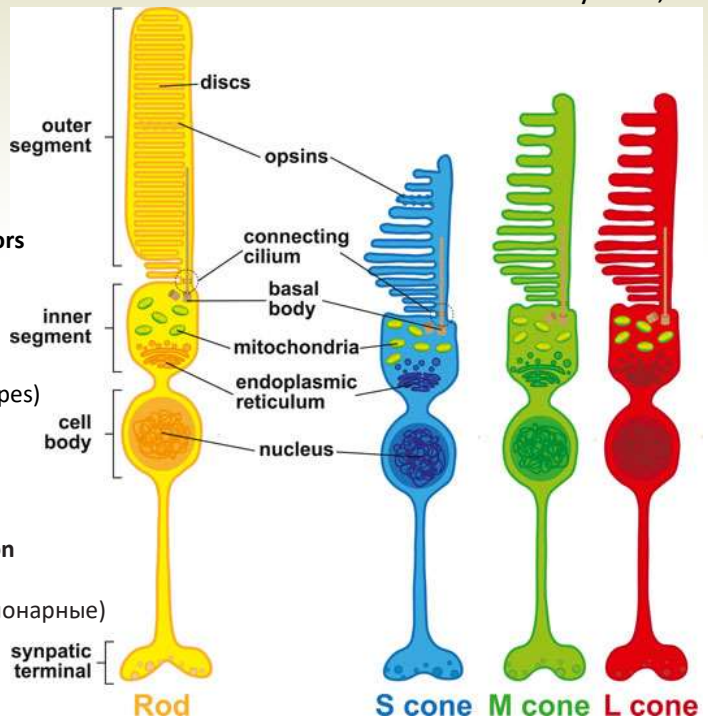

Evolutionary younger

Evolutionary older

Rhodopsin **Opsins**

Mechanisms of opsin delivery into and transport along cone outer segment?

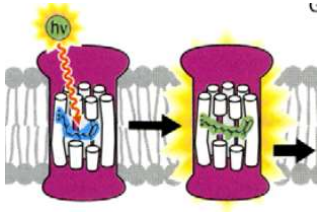

Pugh & Lamb, 2000

Fine structure of outer segments (OS) of rods and cones

Rod OS

Discs are separated, enveloped by the plasma membrane

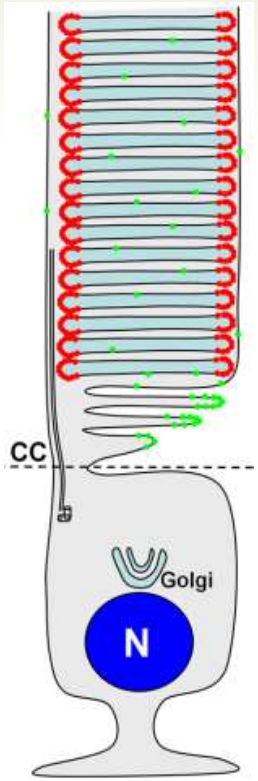

Cone OS

All lamellae and plasma membrane are continuous

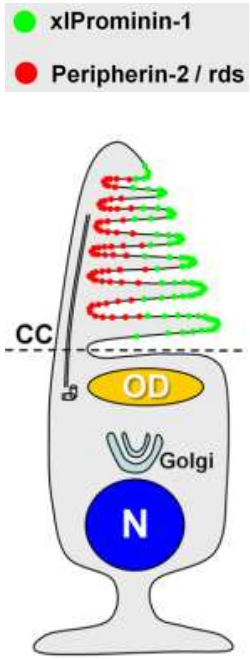

Han, 2012

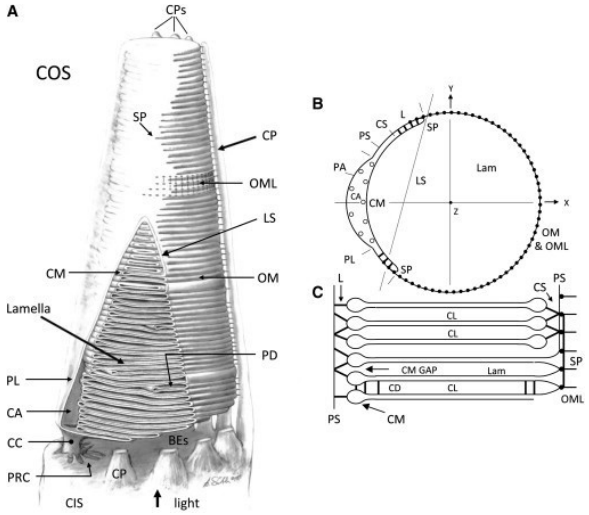

Corless, 2012

Is opsin transport along COS controlled by diffusion or by motor-driven intraflagellar transport (IFT motors) along the axoneme?

Spatial resolution limitations of optical microscopy prevent direct study of OS structure and opsin transport

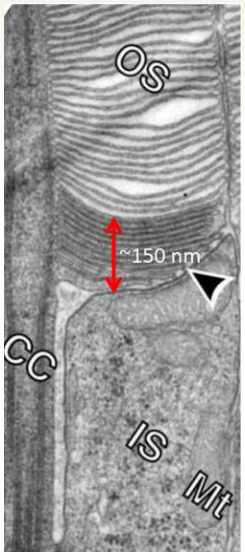

Ding 2015, EM, mice

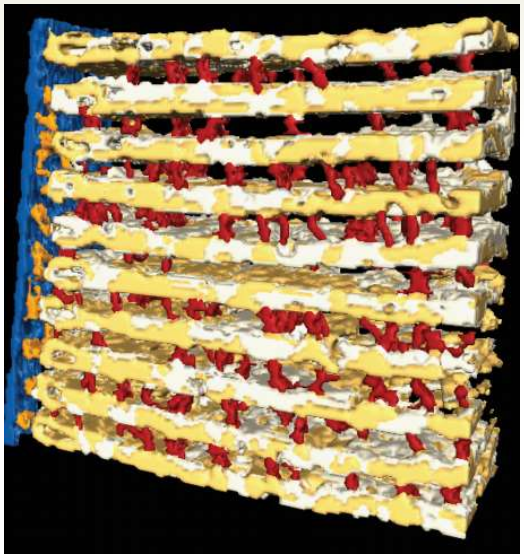

Nickell 2007, Cryo-electron tomography, mice

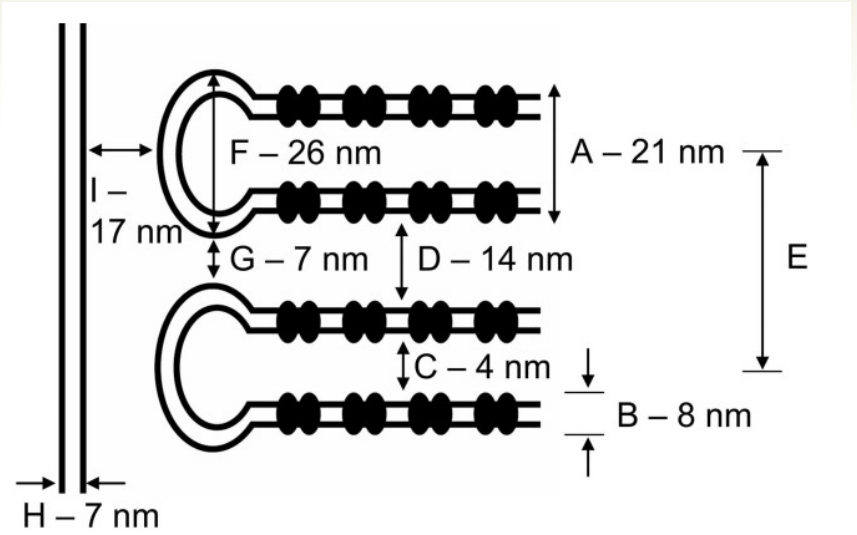

- Diffraction limit of optical microscopy resolution ~500 nm/2 = 250 nm
- Highly non-physiological conditions in EM and cryo-ET preparations

⇒ **To study transport mechanisms in live cells, optical microscopy should be supplemented with quantitative theoretical models**

FRAP experiment in live cones of transgenic *Xenopus laevis* frogs


www.xenbase.org

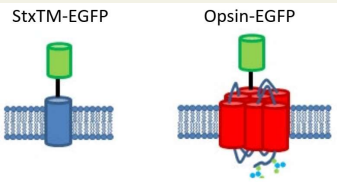

- Fused opsin-GFP and syntaxin-GFP, expressed in *Xenopus laevis* L-cones (expressing red opsin)
- Live cells in retina cuts, frog Ringer's solution, t = 18-20 ^{0}C
- Confocal laser scanning microscopy:

  excitation at 488 nm, detection at 500 nm, bleaching at 920 nm (2P mode)

  spatial resolution $\sigma_{xy} \approx 0.15$ um, $\sigma_z \approx 0.5$ um
- Axial profiles of fluorescence are reconstructed from 3D image stacks

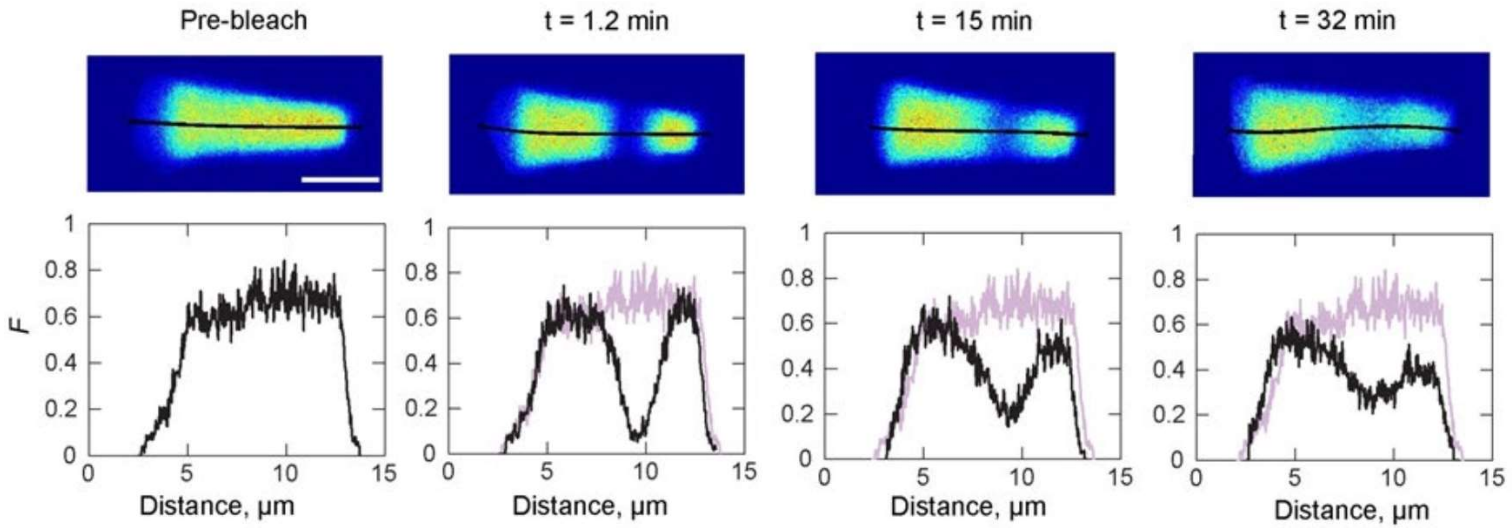

Calvert, 2010

Accurate 3D model

25 lamellae

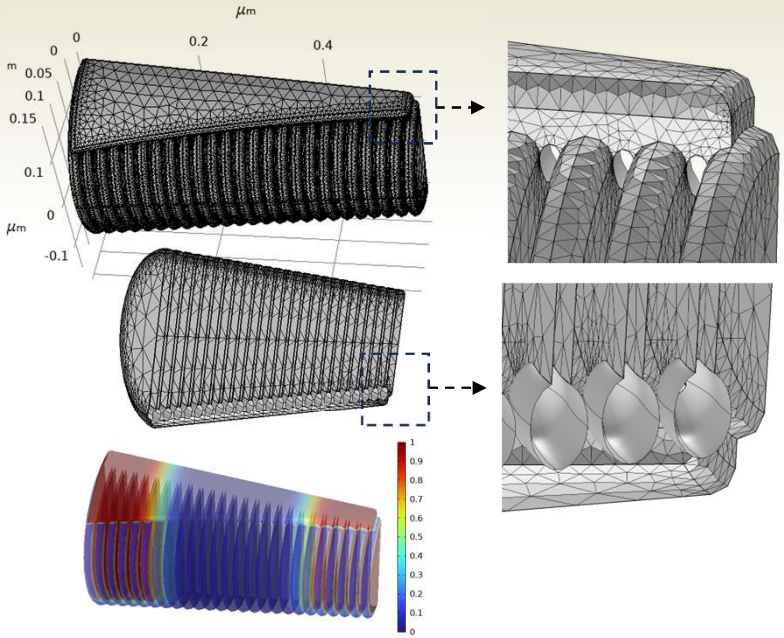

250 lamellae

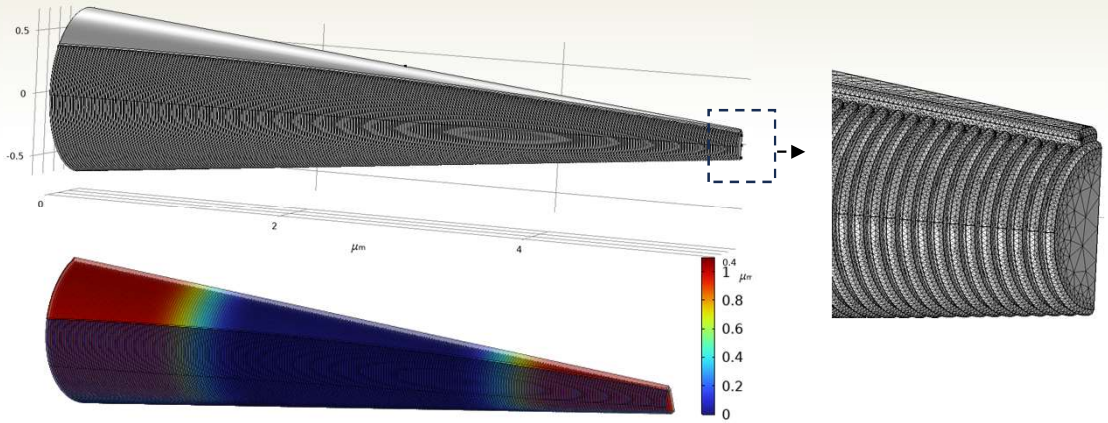

We account for:

- COS lamellar structure
- Impediment of diffusion mobility due to rim structures (HPT, UT) and opsin crowdedness in LS
- Initial photobleaching pattern

Reaction-diffusion equation:

$$\frac{\partial c}{\partial t} = -\nabla\left(-D \cdot \nabla c + c \cdot D \frac{\nabla F_a}{F_a}\right)$$

Reduction from 3D to 1D model

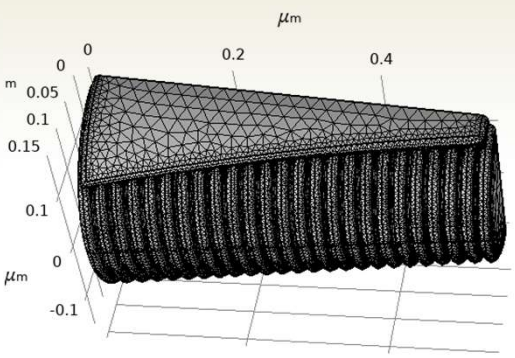

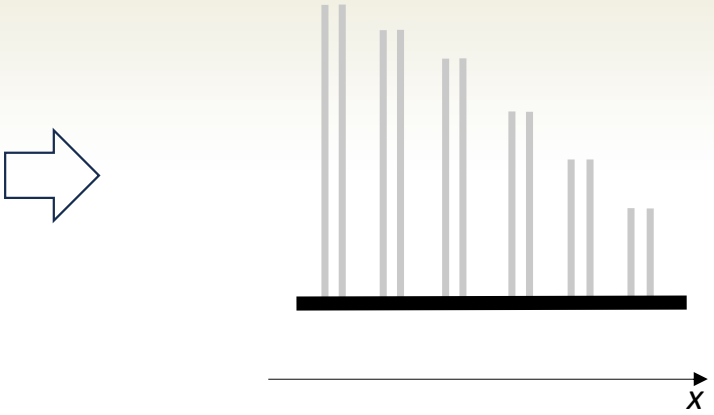

FRAP experiment

To compare with experiment, we account for:

- Signal blurring by the point-spread function (psf)
- psf anisotropy
- COS tilt
- COS width ≤ psf z-size
- Slight movement (bending) of COS during the experiment

Pattern of the flux passing through SP, along PM and along LS

25 lamellae

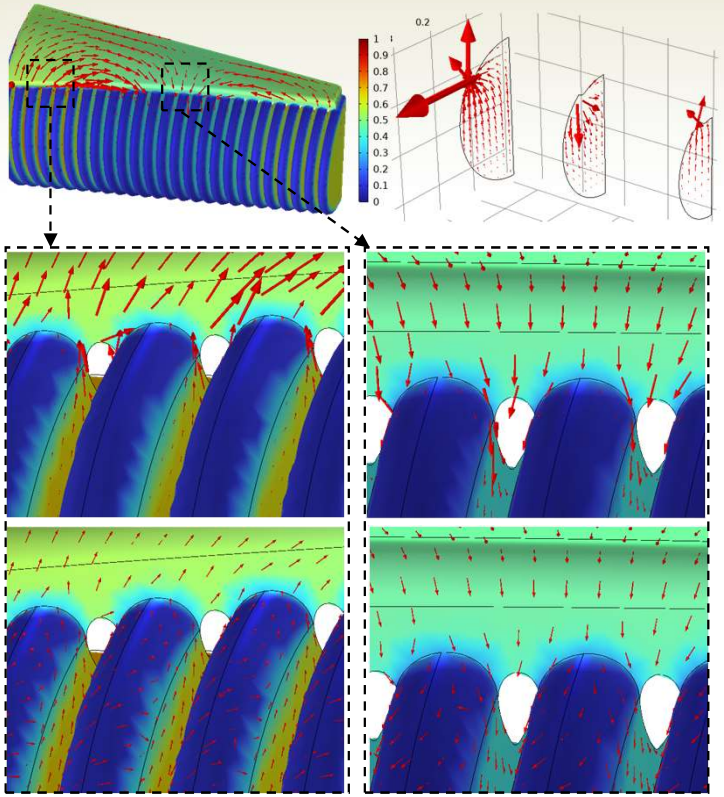

250 lamellae

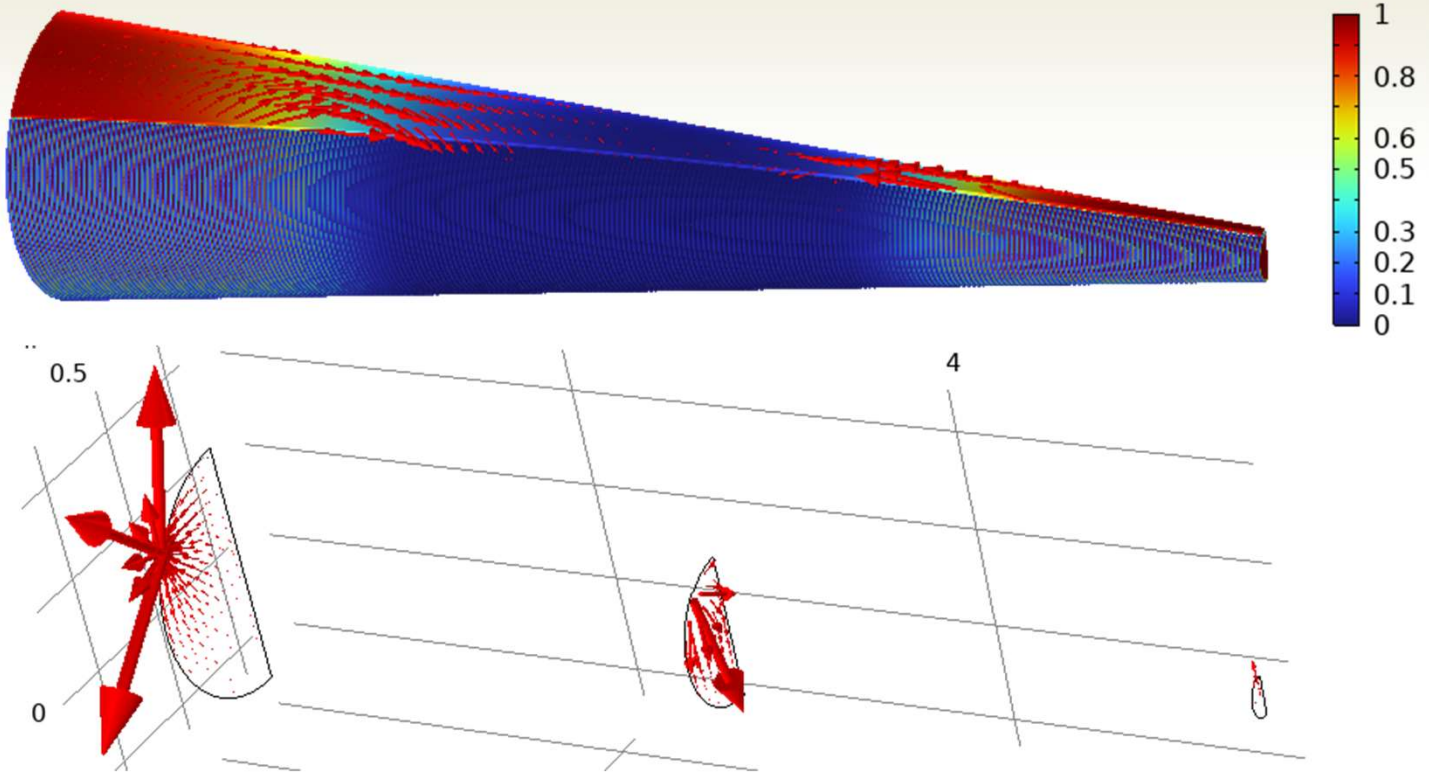

Diffusion control of axial relaxation in 3D model localizes in PM for $N_{lamellae}$ of several dosens and more

Концентрация на оси НС

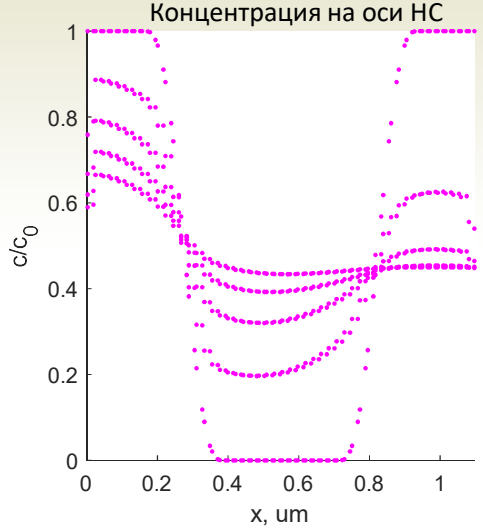

Концентрация в центре НС

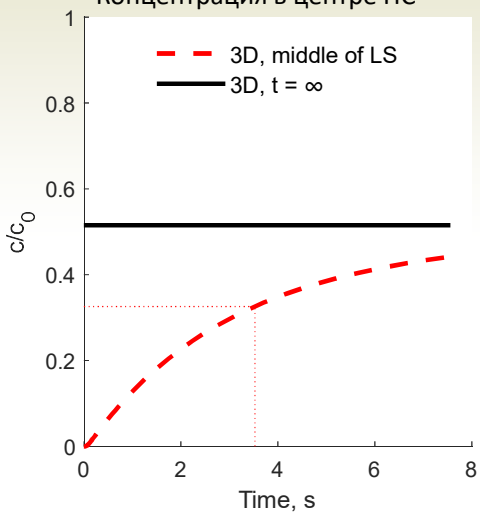

Глобальная чувствительность

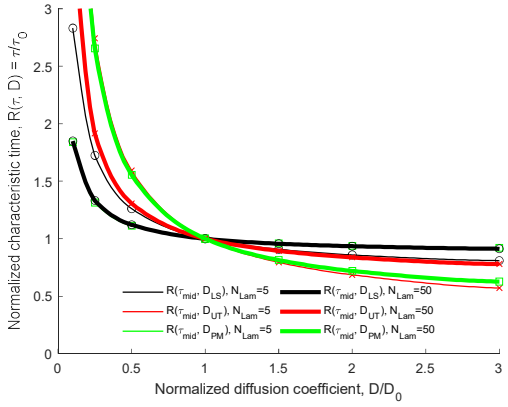

Локальная чувствительность

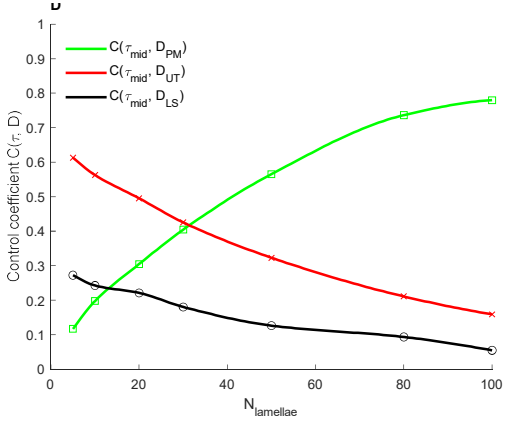

Коэффициент контроля

$$C(\tau, D) = \frac{D}{\tau}\frac{|\Delta\tau|}{\Delta D} = -\frac{D}{\tau}\frac{\Delta\tau}{\Delta D}$$

1D model becomes increasingly good approximation of the 3D model at large $N_{lamellae}$

$N_{lamellae}$=50

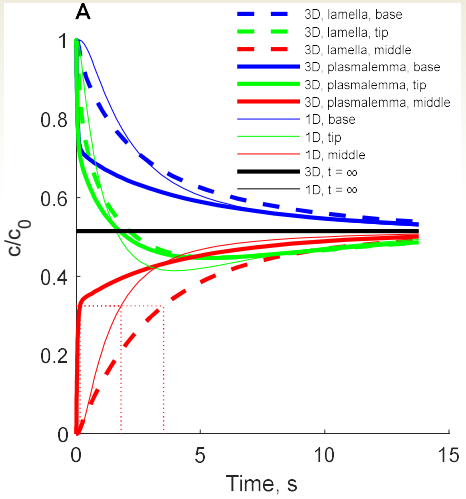

120

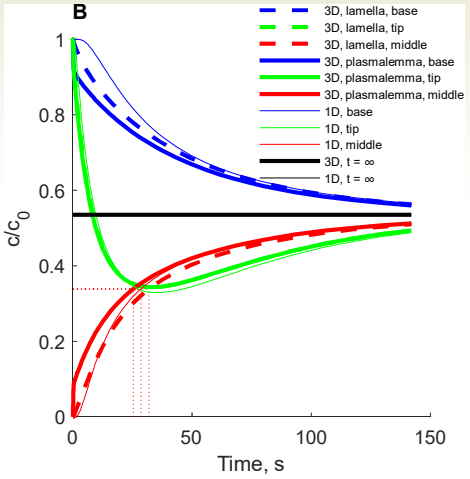

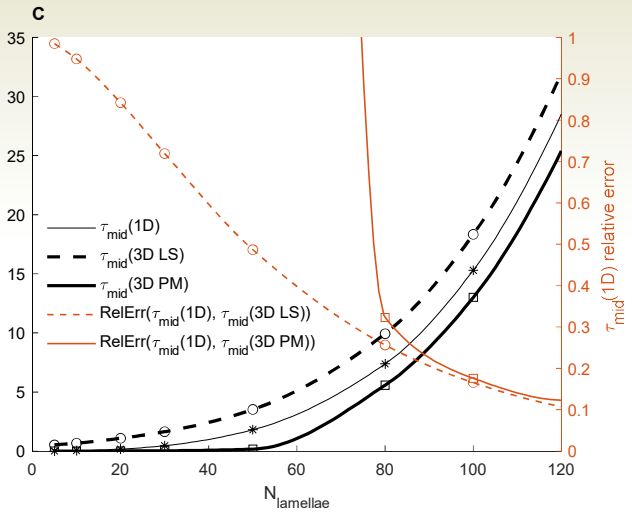

The error of 1D model, that is deviation of 1D from 3D model:

- decreases with increasing N
- is comparable with the difference between LS and PM in 3D model

Fitting 1D model to experimental data

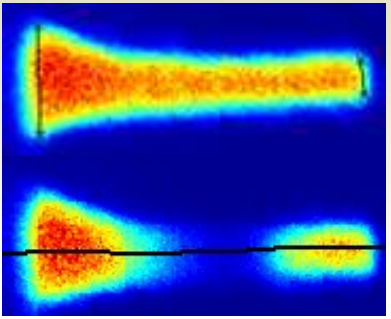

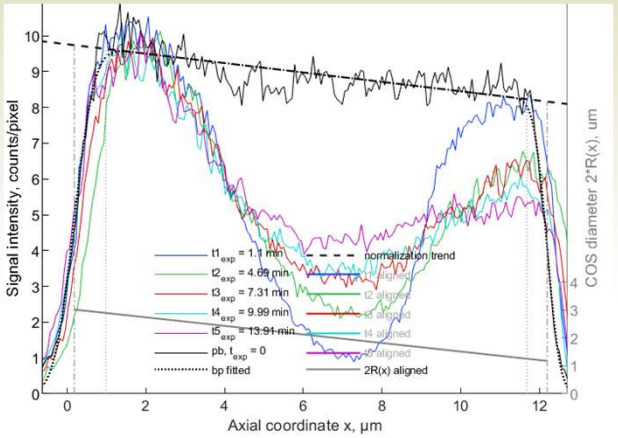

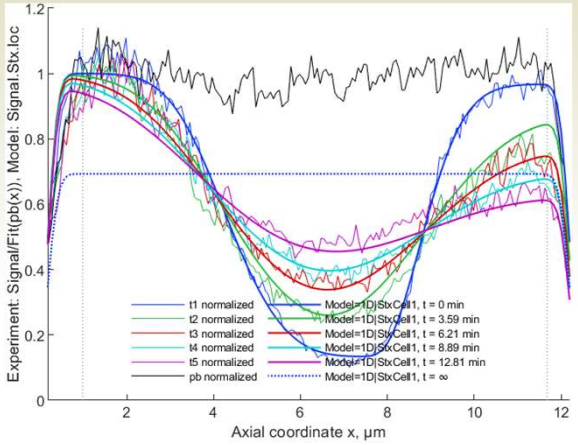

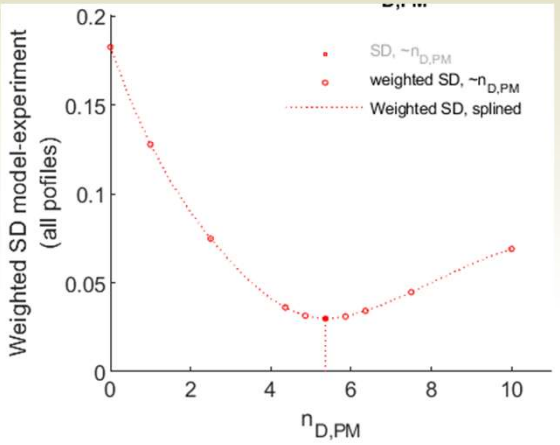

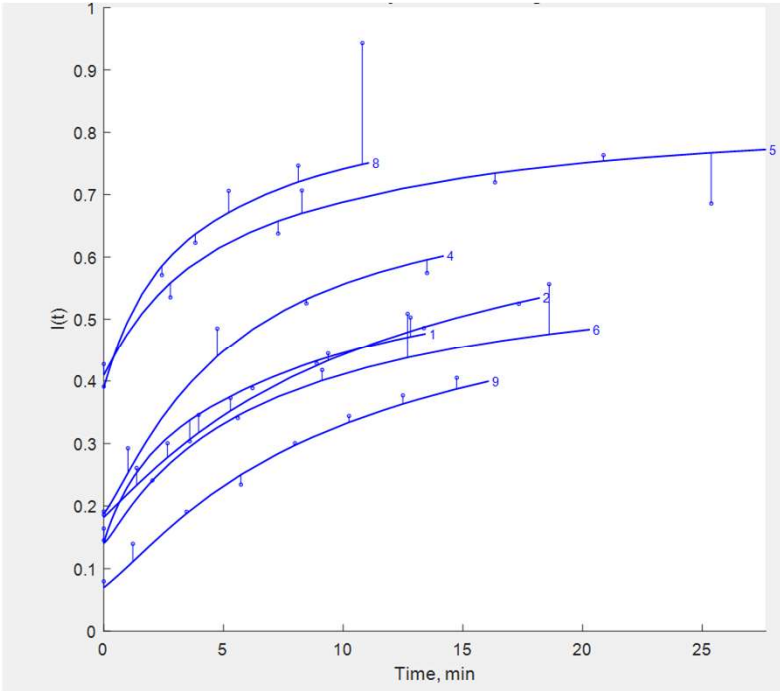

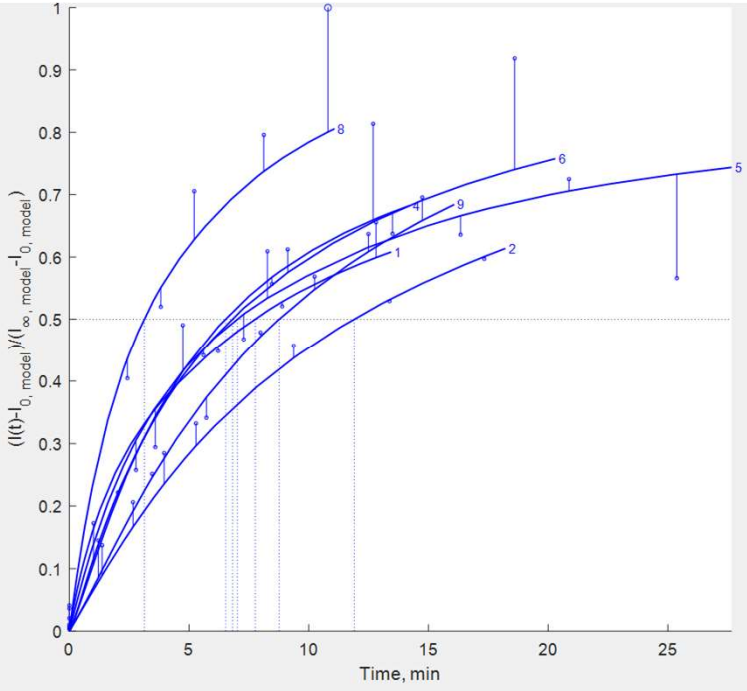

Вывод

Аксиальный транспорт опсина в мембране наружнего сегмента колбочек – между ламеллями – может осуществляться посредством его диффузии вдоль плазматической мембраны, выступающей в качестве шунта.

Участия активного транспорта (везикулы, моторы и т. д.) не требуется.

Этот процесс – пример эффективной клеточной компартментализации, независимой от активного транспорта.